Nanoscale

COMMUNICATION

View Article Online
View Journal | View Issue

Cite this: *Nanoscale*, 2015, **7**, 16590

Received 11th May 2015,
Accepted 11th September 2015

DOI: 10.1039/c5nr03091a

www.rsc.org/nanoscale

Light induced aggregation of specific single walled carbon nanotubes

Madhusudana Gopannagari and Harsh Chaturvedi*

We report optically induced aggregation and consequent separation of specific diameters of nanotubes from stable solutions of pristine single walled carbon nanotubes (SWNTs). Dispersed solutions of pristine SWNTs in different solvents show rapid and selective aggregation. The separated SWNTs show enrichment in specific diameters of SWNTs aggregating under UV, visible and NIR illumination.

Single walled carbon nanotube (SWNT)-based materials have applications in electro-optics, plasmonics, and biotechnology.[1–3] Moreover, dispersion of nanoparticles like one dimensional SWNTs also provides an opportunity to understand the effects of electro-optical forces on intermolecular interactions.[4] SWNTs are commonly dispersed in solution and functionalized with other molecules and polymers for the fabrication of devices and sensors.[5–7] Dispersion of SWNTs produces a mixture of various diameters of metallic and semiconducting SWNTs.[8] Separation of specific SWNTs from solution is an important concern and various methods are being employed including density gradient, gel-chromatography and using surfactants, polymers and other functional molecules.[9–13] Photophoretic forces are predicted to play an important role in chiral and diameter specific separation of SWNTs from solution.[14] We recently reported photophoresis in aggregates of SWNTs in solution.[15] Although optically induced aggregation especially in nanoparticles has theoretically been predicted and reasonably reported, very little experimental proof of aggregation of nanoparticles by light could be found.[16,17] Optically induced aggregation in gold nanoparticles[18] and specifically in SWNTs functionalized with optically active supramolecules has been reported.[19,20] The stability of a solution depends on the dimensions, uniform surface charges and dielectric properties of the interacting particles and solution.[4] Under significant optical excitation, photophoretic forces in resonating particles are expected to affect the colloidal stability, leading to subsequent aggregation of the absorbing SWNTs. Here, we report optically induced aggregation of selective pristine SWNTs from dispersed solution. A well-dispersed, stable solution of pure, pristine SWNTs shows enhanced rates of aggregation under optical illumination by simple UV, broadband visible and NIR light. The optically induced rate of aggregation depends on the frequency and on the intensity of applied illumination. Significantly, the aggregated floc of SWNTs shows enrichment in selective diameters of nanotubes, specific to the frequency of the applied illumination. Hence, we report the phenomenon of optically induced aggregation and its potential application in efficient separation of different diameters of nanotubes from solution. Such optical methods may play an important role in efficient, large scale, non-intrusive separation of specific diameters from pure SWNTs, without any functionalization or creation of defects due to chemical processes.

Well dispersed, stable solutions of pristine SWNTs were prepared by ultrasonication of 0.6 mg of SWNTs (Nano Integris®-IsoNanotubes, 95% purity) in 100 mL of *N*,*N*-dimethylformamide (DMF) (Sigma Aldrich®). The pristine SWNTs have a diameter distribution from ~0.7 nm to 1.7 nm, and the average length is expected to be 300 nm to 1.7 nm. Solutions were found stable for weeks. Care was taken to avoid water absorption and light exposure. Stable solutions of dispersed pristine SWNTs were exposed to UV light (125 W, 352 nm), broadband visible light (125 Watts) and NIR light (Fuzi, 150 Watts) for 30–240 min. Control samples were kept in the dark for the same time and were used to calculate the normalized rate of aggregation for SWNTs in the presence of light. The samples kept in light and in the dark were centrifuged @ 8000 rpm (Eppendorf® Mini Spin Centrifuge Machine) for 10 min to carefully separate the supernatant from the solution. The separated supernatant and flocs were analyzed by using a UV-Vis-NIR spectrophotometer (Perkin Elmer® Lambda 950 UV-Vis spectrometer) and a Raman spectrometer (632 nm laser).

The absorption spectra of pure SWNTs show cumulative absorption by different diameters of nanotubes in solution. As shown in Fig. 1, the absorption spectra of pure SWNTs show

Department of Physics, Indian Institute of Science Education and Research, Pune-411008, India. E-mail: hchaturv@iiserpune.ac.in

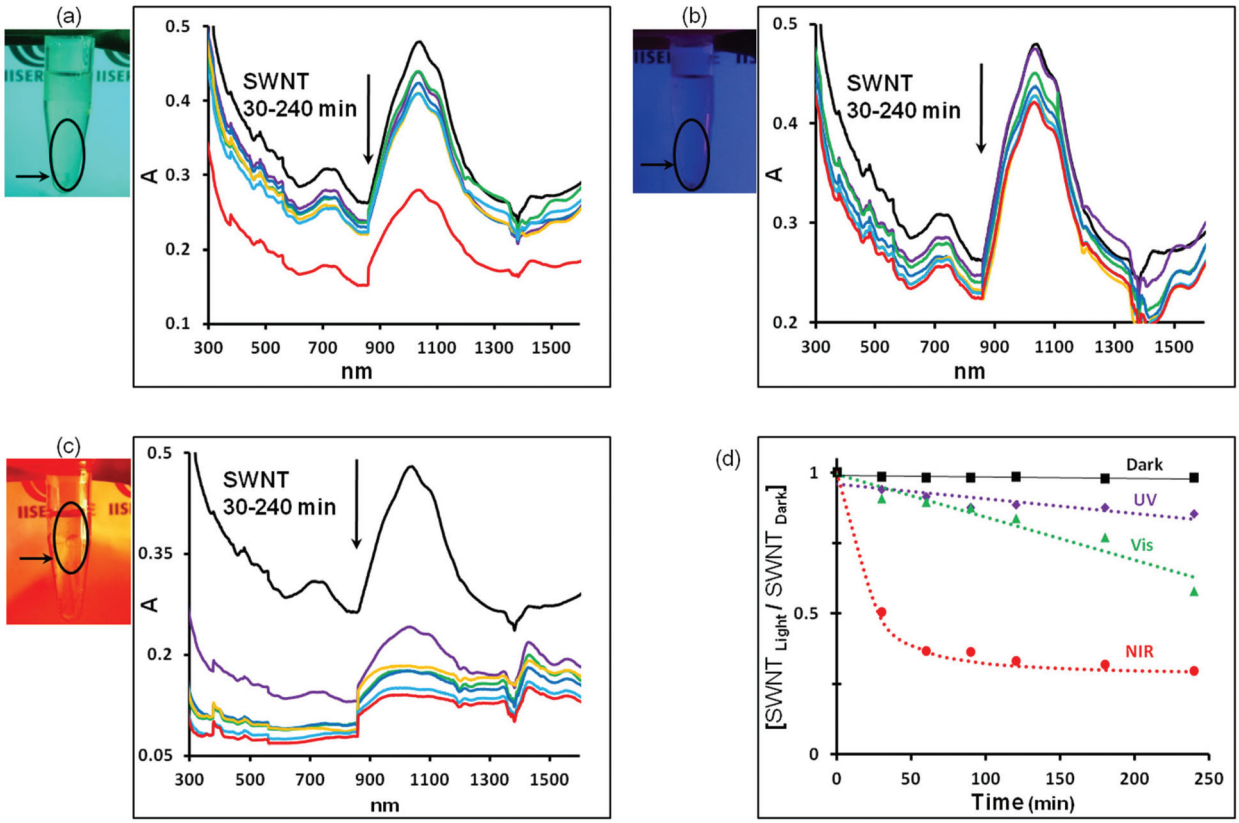

Fig. 1 Light induced aggregation under broadband visible (a), UV (b) and NIR lamps (c) are shown. After 240 min illumination time, aggregated flocs are shown by an arrow. The absorption spectra of the supernatant collected from pure SWNTs under UV, visible and NIR lamps show consistent decrease in concentration when exposed to varying durations from 30 min to 240 min; (d) shows a relative rate of optically induced aggregation in pristine SWNTs under UV, visible and NIR illumination.

the background plasmonic resonance in UV (300–450 nm) due to the metallic SWNTs and van Hove singularities due to band-gap absorption in the visible and NIR regions by the semiconducting SWNTs. Absorption by the pristine SWNTs in the NIR frequency (850–1400 nm) is attributed to the S_{11} band-gap absorption by the semiconducting SWNTs of specific diameters.[21] Individual absorption peak intensities representing electronic transitions in the NIR S_{11} band of semiconducting SWNTs are sensitive to the relative concentration of SWNTs with specific tube diameters and chirality. Along with a consistent decrease in the concentration of the separated supernatant of pristine SWNTs by varying the time of optical exposure, indicating optically induced aggregation, Fig. 1(a–c) also show discernible changes in both the UV and in the visible–NIR frequency of the supernatant suggesting selective aggregation of different diameters of SWNTs. The supernatants separated from the solution and exposed to NIR illumination for different times (Fig. 1c) distinctly show consistent changes and enrichment with specific diameters of SWNTs. Optically induced aggregation was observed for pristine SWNTs exposed to broadband visible, UV and NIR illumination. The rate of optically induced aggregation was determined using absorption spectroscopy as shown in Fig. 1(a–c). The concentration of each supernatant was normalized with reference to the stable concentration of the sample kept in the dark. The concentration at 840 nm was used to determine the rate of aggregation as the spectra here are relatively flat and free of van Hove singularities. The rate of aggregation was plotted with respect to the time of exposure for each sample under different lamps. At the maximum exposure time of 240 minutes, about 20% and 40% of SWNT aggregate under UV and broadband visible illumination respectively, however rapid aggregation was observed under NIR illumination with 65% SWNTs aggregating, as shown in Fig. 1(d).

This phenomenon of optically induced aggregation of pristine SWNTs in DMF was further studied using pre-separated 95% pure metallic and semiconducting SWNTs. The pre-separated SWNTs were bought from NanoIntegris and were dispersed in DMF without any further modifications. Along with the dispersion of SWNTs in DMF, stable solutions of pristine SWNTs in NMP and chloroform were also prepared, by a similar method of ultra-sonication as reported above. Rapid aggregation of SWNTs was observed in each of the SWNT solutions under broadband (UV-Vis) illumination. The metallic SWNTs show a higher rate of aggregation than the semiconducting or pristine SWNTs as shown in Fig. 2(a).

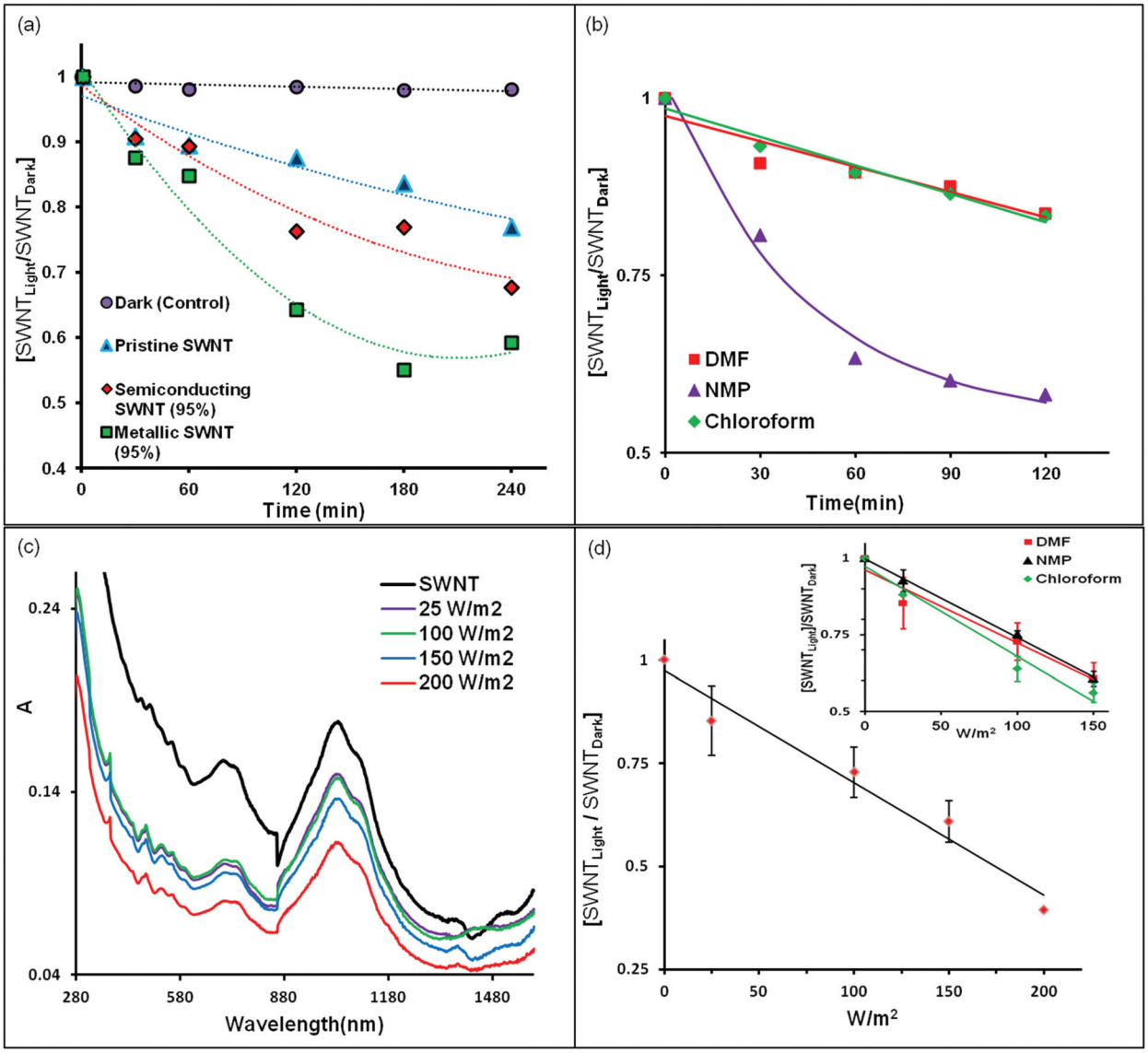

Fig. 2 (a) Light induced rate aggregation in pristine (un-separated), semiconducting (95% pure) and metallic (95% pure) SWNTs in DMF, under broadband visible illumination. (b) Optically enhanced rates of aggregation in different solvents. (c) Absorption spectra of the supernatant, separated from the pristine SWNTs after exposure to visible light illumination for varying intensities. (d) SWNTs dispersed in DMF showing a rapid increase in the rate of aggregation with an increase in the visible intensity. Inset: SWNTs dispersed in NMP and chloroform showing similar rates of optically induced aggregation as in DMF.

Un-separated pure SWNTs dispersed in different organic solvents (DMF, NMP, and chloroform) were exposed to a broadband halogen lamp for varying time intervals (30–240 min). The samples were then centrifuged and the supernatants were separated from the aggregated SWNTs. Similar to the optically induced aggregation observed in DMF, the supernatants separated from the SWNTs dispersed in NMP and chloroform show consistent decrease in the concentration of SWNTs with the corresponding increase in the exposure time. The concentration of the SWNTs in the supernatant was normalized with the stable pristine SWNT solution, kept in the dark (control). The corresponding graph plotted in Fig. 2(b) shows a similar optically induced rate of aggregation for NMP and DMF, however the rate of aggregation is found to be 20% more rapid in the case of SWNTs dispersed in chloroform. Experiments show that the optically induced aggregation in SWNTs depends on the type of the SWNTs (metallic and semiconducting) and the solvent used.

This phenomenon of optically induced aggregation was further studied by varying the intensities of the visible light. A solution of SWNTs dispersed in each of the organic solvents (DMF, NMP and chloroform) was exposed to visible light for 1 hour with varying intensities (25–150 W m^{-2}). Fig. 2(c) shows the absorption spectra of the supernatant separated from the optically aggregated SWNTs in DMF solution. As shown in Fig. 2(d), the concentration of SWNTs dispersed in all three

organic solvents (DMF, NMP and chloroform) shows a linearly enhanced rate of aggregation, with the corresponding increase in the intensity of visible light illumination. Interestingly when exposed for varying time intervals, the SWNTs dispersed in chloroform show much rapid aggregation as compared to the SWNTs dispersed in NMP and DMF; however, for different intensities of the same visible light illumination, the SWNTs in all the three solvents show a similar rate of aggregation.

The diameter (d_t) of the semiconducting SWNTs may be calculated using the absorption in the NIR frequency (λ_{11} by $\lambda_{11} = \frac{hcd_t}{2a_{c-c}\gamma_0}$, where the C–C bond distance is measured to be 0.142 nm, and γ_0 = 2.7 eV is the interaction energy.[22] Fig. 3(a) shows substantial differences in the absorption spectra of the supernatant and aggregated flocs, separated from the solution of pristine SWNTs, after exposing to NIR illumination for 240 min. Significant changes in the normalized NIR band (850–1500 nm) of the separated supernatant and flocs are shown in Fig. 3(a) [left inset]. Variations in the NIR peak intensity and frequency are associated with the changes in the relative distribution of the different diameters of the semiconducting SWNTs in the solution. The histogram in Fig. 3(a) [right inset] shows relative enrichment in different diameters of semiconducting SWNTs in the separated supernatant and the optically aggregated floc. This distribution of different diameters of semiconducting SWNTs in a solution is calculated by fitting multiple the Lorentzian peaks to the normalized absorption in the NIR frequency (900–1400 nm). While the diameter of SWNTs is estimated by the frequency of the peak, the intensity of the normalized peaks depends on the relative enrichment of SWNTs of that specific diameter.

An exponential increase in the background absorption of pristine SWNTs in the UV-visible range (300–500 nm) is attributed to the plasmonic resonance due to the metallic SWNTs. An extinction co-efficient for each of the absorption spectra in Fig. 1(c) was calculated by exponential fits in the 300–500 nm frequency range. Fig. 3(b) shows different exponential fits to the absorption spectra of the supernatant and aggregated flocs, separated from the pristine SWNTs after NIR illumination for 240 min. The inset in Fig. 3(b) shows a consistent increase in the extinction coefficient of the separated supernatant with an increase in the time of exposure to NIR

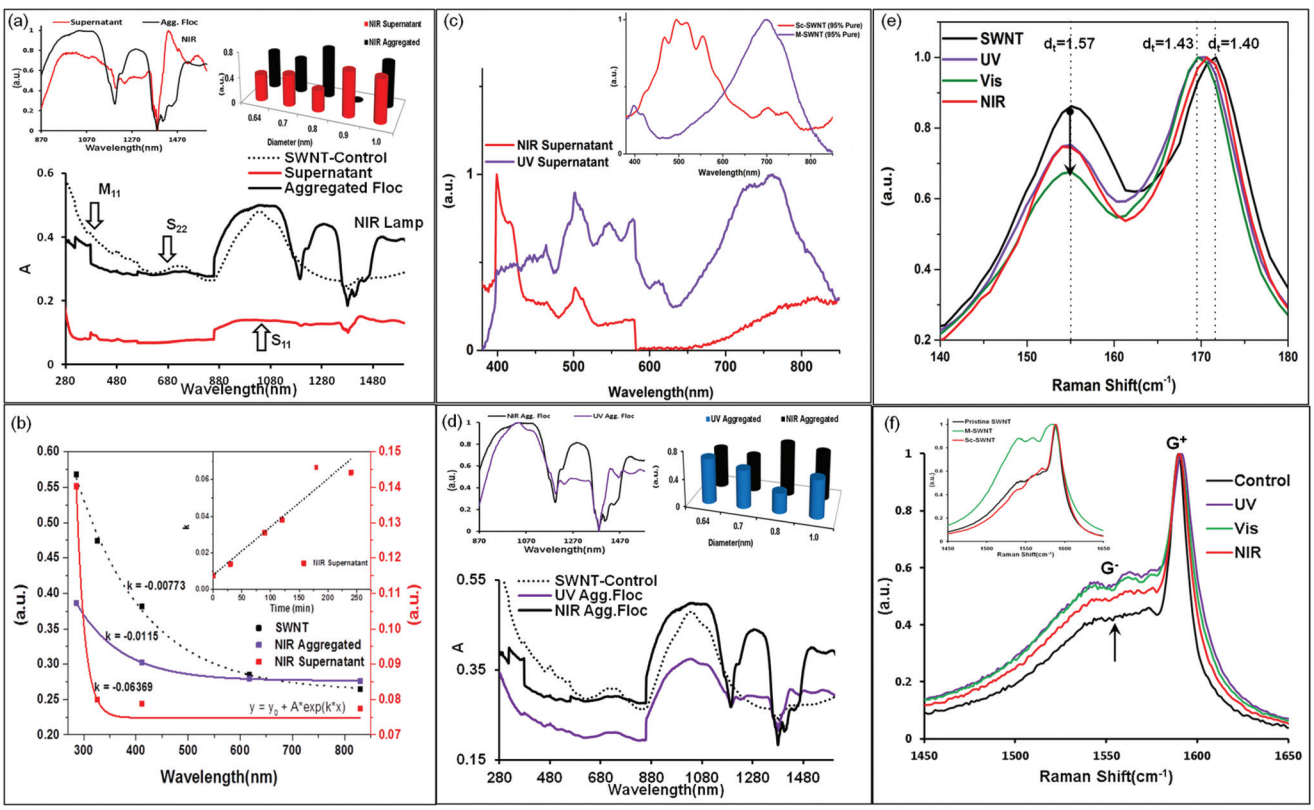

Fig. 3 (a) Absorption spectra of the supernatant and aggregated flocs as separated from the pristine SWNT (dotted line) after 240 min exposure to NIR illumination and normalized NIR bands (left inset). Histogram showing enrichment of specific diameters in the separated supernatant and aggregated SWNTs; (b) shows increase in the extinction coefficient (k) of SWNTs in the supernatant with an increase in the time of exposure to NIR illumination. (c) Normalized absorption spectra of the supernatants separated from the pristine SWNT solution after UV and NIR illumination. Inset shows the absorption spectra for reference solution of pre-separated, pure metallic and semiconducting SWNTs. (d) Absorption spectra of aggregated flocs under UV and NIR light illumination and normalized NIR bands (left inset). Histogram showing enrichment in specific diameters (e) shows RBM (d) G band Raman spectra of optically aggregated SWNTs, exposed to UV, visible and NIR illumination.

illumination. This consistent increase in the extinction coefficient of the separated supernatant indicates the corresponding decrease in the plasmonic resonance due to the metallic SWNTs. The absorption spectra of the supernatant separated after NIR exposure for 30 min–240 min (Fig. 1(a)) show a consistent loss of background resonance indicating the aggregation of metallic SWNTs and increase in the specific diameters of the semiconducting SWNTs in the separated supernatant. The exponential background absorption due to the plasmonic resonance by metallic SWNTs was subtracted from the absorption spectra of the supernatants separated after exposure to NIR and UV illumination for 240 min. With the background plasmonic absorption subtracted, Fig. 3(c) shows sharp van Hove singularities due to the band gap absorption by the semiconducting SWNTs of different diameters. Significant discernible changes are observed in the absorption peaks of the supernatants of pristine SWNTs separated after UV and NIR illumination. The inset in Fig. 3(c) shows absorption peaks from the reference solution of metallic (95% pure) and semiconducting SWNTs (95% pure). The supernatant separated after exposure to NIR illumination shows a significant enrichment in specific diameters of SWNTs absorbing at 400 nm; whereas, the supernatant separated from UV exposure shows a significant enrichment in SWNTs absorbing at around 750 nm. By comparing the absorption spectra of the optically separated supernatants with the reference solution of pure metallic and semiconducting SWNTs, it is inferred that the supernatant separated after NIR illumination shows an enrichment in selective diameters of semiconducting SWNTs whereas, the supernatant separated after UV exposure shows an enrichment in specific diameters of metallic SWNTs.

Similar to Fig. 3(a), Fig. 3(d) compares the diameter distribution in the SWNTs aggregating under UV and NIR illumination. Discernible changes are also observed in the Radial Breathing Mode (RBM) (Fig. 3e) and G band (Fig. 3f) Raman spectra of the optically aggregated flocs separated from the pristine SWNTs after exposure to UV, visible and NIR illumination.

The RBM of pristine SWNTs depends on the diameter of the nanotube.[23] The RBM of the aggregated SWNTs under different illuminations shows distinct enrichment of specific diameters of SWNTs which can be calculated using the relationship $\omega_{RBM} = (\alpha_{RBM}/d) + \alpha_{bundle}$,[21] where α_{RBM}, α_{bundle} are the constants associated with the bundling effect and scaling factor in the RBM spectra of nanotubes respectively and d is the diameter of the SWNT corresponding to the RBM peak frequency (ω_{RBM}). As calculated from the expression, the RBM of aggregates shows relative enrichment in the following diameters 1.42, 1.43, and 1.41 nm when exposed to UV, visible or NIR illumination respectively. Consequent changes are also seen in SWNTs with a larger diameter of 1.57 nm corresponding to the RBM frequency of ~155 cm^{-1}. The changes in the G band Raman spectra of pristine SWNTs indicate significant changes in the relative concentration of metallic and semiconducting SWNTs.[24,25] Fig. 3(f) shows considerable changes in the normalized G^- band, indicating an increase in the metallic SWNTs aggregating under UV, visible and NIR illumination as compared to pristine SWNT solution. In the G-band Raman spectra of the reference, the pre-separated metallic and semiconducting SWNTs are shown in Fig. 3(f) (inset). The inset shows a considerable increase in the G^- band for the metallic SWNTs (95%) as compared to the semiconducting SWNTs (95%). Hence, the RBM and G band Raman spectra do indicate enrichment in the aggregating SWNTs of specific diameters and changes in the ratio of metallic and semiconducting SWNTs depending on the frequency of optical illumination.

This phenomenon of optically induced aggregation in selective SWNTs may be due to photophoretic and photo-thermal processes in SWNTs.[26] Induced photophoretic motion by similar lamps in aggregates of metallic and semiconducting SWNTs have recently been reported.[15] Similar photophoretic forces along with photo-thermal processes may be responsible for selective aggregation of pristine SWNTs. Even with inherent limitations due to various assumptions of surface charges, geometry and dielectrics, the aggregation of SWNT dispersions is still widely explained using the conventional DLVO theory.[28–30] The DLVO theory describes total interaction energy between two particles in solution as a net result of the attractive van der Waals (vdW) forces and the repulsive electrostatic double-layer (EDL) interactions (Fig. 4). This interaction potential

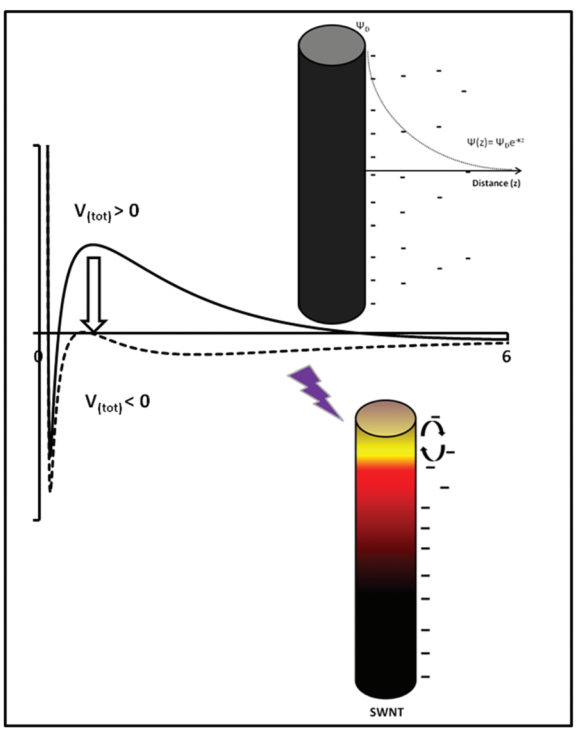

Fig. 4 Conceptual model of optically induced aggregation of SWNTs from solution. The figure shows interaction potential between cylinders according to the DLVO theory. Uniform surface charges are shown to be affected by illumination in an absorbing SWNT; leading to colloidal instability.

barrier, which defines the colloidal stability conventionally, depends on the dimensions, dielectrics and surface charges at the particle–solution interface. For, $V_{tot} < 0$, the van-der Waals attractive term is greater than the repulsive EDL leading to colloidal instability and aggregation of the particles. Our experiments show a significant decrease in V_{tot} under optical illumination leading to an enhanced rate of aggregation.

The total potential (V_{tot}) of two interacting cylinders in solution is approximated by the following expression:[4]

$$V_{tot} = \left(\frac{-A_H}{12\sqrt{2}D^{3/2}} + \frac{k^{1/2}}{\sqrt{2\pi}} Ze^{-kD}\right)\left[\sqrt{\frac{R_1R_2}{R_1+R_2}}\right]$$

where D is the surface distance between two nanotubes with radius R_1 and R_2. A_H is the Hamaker constant in the attractive van der Waals contribution and Z is the interaction constant of the repulsive EDL term, $k^{1/2}$ being measure of Debye length (k^{-1}). According to the DLVO theory, surface charges are considered uniform at either constant surface potential or constant charge density. Both the photo-thermal and photophoretic forces depend on the absorption of the particles. Local kinetics and non-uniformity of the surface charges in the absorbing SWNTs may affect the interaction potential leading to colloidal instability and aggregation. Thermal gradient on the surface of an absorbing particle in resonant optical frequency is given as $\nabla\hat{T} = \frac{1}{k_p}\hat{Q}_p$, where k_p is the internal heat conductivity of the particle and $\hat{Q}_p$ is volumetric thermal energy which depends on the refractive index of the absorbing particle.[27] It is expected that absorption and plasmonic resonance may lead to local temperature variations depending on the thermal conductivity of the absorbing SWNTs. Since absorption by the SWNTs depends on the diameter of the SWNTs, the absorbing SWNTs of selective diameters are expected to have enhanced photo-thermal and photophoretic effects. Clearly, more research is needed, both theoretically and experimentally to better understand the phenomenon.

However, in conclusion we report the phenomenon of optically induced aggregation in selective SWNTs from pristine well dispersed solution, thereby causing separation of specific SWNTs. Rapid aggregation was observed for pure SWNT solution exposed to optical illumination by simple light sources. The results show that the rate of aggregation primarily depends on the intensity of light with selective aggregation in specific SWNTs due to the illumination frequency. Our results show that controlled optical excitation may be used for large scale efficient separation of particular diameters of SWNTs. The absorption and Raman spectra of the separated supernatant and aggregated flocs especially under NIR illumination show relative enrichment in specific SWNTs. Additional theoretical and experimental research should provide deeper fundamental understanding of the phenomenon and initiate the development of efficient optical processes for separation of not just specific diameter SWNTs, but possibly of other nanoparticles from the solutions too.

Acknowledgements

The authors are deeply indebted to Ramanujan fellowship (SR/S2/RJN-28/2009) and funding agencies DST (DST/TSG/PT/2012/66) and Nanomission (SR/NM/NS-15/2012) for generous grants.

References

1 P. Avouris, M. Freitag and V. Perebeinos, Carbon-nanotube photonics and optoelectronics, *Nat. Photonics*, 2008, **2**(6), 341–350.
2 E. Bekyarova, Y. Ni, E. B. Malarkey, V. Montana, J. L. McWilliams, R. C. Haddon and V. Parpura, Applications of carbon nanotubes in biotechnology and biomedicine, *J. Biomed. Nanotechnol.*, 2005, **1**(1), 3.
3 W. Hu, Z. Lu, Y. Liu and C. M. Li, In situ surface plasmon resonance investigation of the assembly process of multiwalled carbon nanotubes on an alkanethiol self-assembled monolayer for efficient protein immobilization and detection, *Langmuir*, 2010, **26**(11), 8386–8391.
4 J. N. Israelachvili, *Intermolecular and surface forces: revised third edition*, Academic press, 2011.
5 C. A. Mitchell, J. L. Bahr, S. Arepalli, J. M. Tour and R. Krishnamoorti, Dispersion of functionalized carbon nanotubes in polystyrene, *Macromolecules*, 2002, **35**(23), 8825–8830.
6 S. Huang, Q. Fu, L. An and J. Liu, Growth of aligned SWNT arrays from water-soluble molecular clusters for nanotube device fabrication, *Phys. Chem. Chem. Phys.*, 2004, **6**(6), 1077–1079.
7 J. Li, Y. Lu, Q. Ye, M. Cinke, J. Han and M. Meyyappan, Carbon nanotube sensors for gas and organic vapor detection, *Nano Lett.*, 2003, **3**(7), 929–933.
8 Z. Chen, X. Du, M.-H. Du, C. D. Rancken, H.-P. Cheng and A. G. Rinzler, Bulk Separative Enrichment in Metallic or Semiconducting Single-Walled Carbon Nanotubes, *Nano Lett.*, 2003, **3**(9), 1245–1249.
9 Y. Maeda, S.-i. Kimura, M. Kanda, Y. Hirashima, T. Hasegawa, T. Wakahara, Y. Lian, T. Nakahodo, T. Tsuchiya and T. Akasaka, Large-scale separation of metallic and semiconducting single-walled carbon nanotubes, *J. Am. Chem. Soc.*, 2005, **127**(29), 10287–10290.
10 M. Zheng, A. Jagota, E. D. Semke, B. A. Diner, R. S. McLean, S. R. Lustig, R. E. Richardson and N. G. Tassi, DNA-assisted dispersion and separation of carbon nanotubes, *Nat. Mater.*, 2003, **2**(5), 338–342.
11 C. Ménard-Moyon, N. Izard, E. Doris and C. Mioskowski, Separation of semiconducting from metallic carbon nanotubes by selective functionalization with azomethine ylides, *J. Am. Chem. Soc.*, 2006, **128**(20), 6552–6553.
12 H. Liu, D. Nishide, T. Tanaka and H. Kataura, Large-scale single-chirality separation of single-wall carbon nanotubes by simple gel chromatography, *Nat. Commun.*, 2011, **2**, 309.
13 M. S. Arnold, A. A. Green, J. F. Hulvat, S. I. Stupp and M. C. Hersam, Sorting carbon nanotubes by electronic

structure using density differentiation, *Nat. Nanotechnol.*, 2006, **1**(1), 60–65.
14 D. Smith, C. Woods, A. Seddon and H. Hoerber, Photophoretic separation of single-walled carbon nanotubes: a novel approach to selective chiral sorting, *Phys. Chem. Chem. Phys.*, 2014, **16**(11), 5221–5228.
15 G. Madhusudana, V. Bakaraju and H. Chaturvedi, Photophoresis in Single Walled Carbon Nanotubes, arXiv preprint arXiv:1503.07353, 2015.
16 H. Eckstein and U. Kreibig, Light induced aggregation of metal clusters, *Z. Phys. D: At., Mol. Clusters*, 1993, **26**(1), 239–241.
17 V. P. Drachev, S. V. Perminov and S. G. Rautian, Optics of metal nanoparticle aggregates with light induced motion, *Opt. Express*, 2007, **15**(14), 8639–8648.
18 N. Satoh, H. Hasegawa, K. Tsujii and K. Kimura, Photoinduced coagulation of Au nanocolloids, *J. Phys. Chem.*, 1994, **98**(8), 2143–2147.
19 H. Chaturvedi and J. Poler, Photon enhanced aggregation of single walled carbon nanotube dispersions, *Appl. Phys. Lett.*, 2007, **90**(22), 223109.
20 A. Sharma, E. S. Prasad and H. Chaturvedi, Optically Induced Aggregation In Single Walled Carbon Nanotubes Functionalized with Bacteriorhodopsin, arXiv preprint arXiv:1503.05719, 2015.
21 S. M. Bachilo, M. S. Strano, C. Kittrell, R. H. Hauge, R. E. Smalley and R. B. Weisman, Structure-assigned optical spectra of single-walled carbon nanotubes, *Science*, 2002, **298**(5602), 2361–2366.
22 J. W. Wilder, L. C. Venema, A. G. Rinzler, R. E. Smalley and C. Dekker, Electronic structure of atomically resolved carbon nanotubes, *Nature*, 1998, **391**(6662), 59–62.
23 M. S. Dresselhaus, G. Dresselhaus, R. Saito and A. Jorio, Raman spectroscopy of carbon nanotubes, *Phys. Rep.*, 2005, **409**(2), 47–99.
24 M. Dresselhaus, R. Saito and A. Jorio, Semiconducting carbon nanotubes, *Phys. Semicond., A*, 2005, **772**, 25–31.
25 S. D. M. Brown, A. Jorio, P. Corio, M. S. Dresselhaus, G. Dresselhaus, R. Saito and K. Kneipp, Origin of the Breit-Wigner-Fano lineshape of the tangential \textit{G} -band feature of metallic carbon nanotubes, *Phys. Rev. B: Condens. Matter*, 2001, **63**(15), 155414.
26 T. Murakami, H. Nakatsuji, M. Inada, Y. Matoba, T. Umeyama, M. Tsujimoto, S. Isoda, M. Hashida and H. Imahori, Photodynamic and photothermal effects of semiconducting and metallic-enriched single-walled carbon nanotubes, *J. Am. Chem. Soc.*, 2012, **134**(43), 17862–17865.
27 H. J. Keh and H. J. Tu, Thermophoresis and photophoresis of cylindrical particles, *Colloids Surf., A*, 2001, **176**(2), 213–223.
28 E. Verwey and J. Overbeek, *Theory of the stability of lyophobic colloids*, Elsevier Pub. Co., New York, 1948.
29 B. Derjaguin and L. Landau, Theory of the stability of strongly charged lyophobic sols and of the adhesion of strongly charged particles in solutions of electrolytes, *Prog. Surf. Sci.*, 1993, **43**(1), 30–59.
30 H. Sonntag, K. Strenge, B. Vincent and B. Vincent, *Coagulation kinetics and structure formation*, Springer, US, 1987.

